JOURNAL OF MATERIALS SCIENCE **40** (2005) 1371–1376

Composition and annealing effects in polythiophene/fullerene solar cells

Y. KIM*, S. A. CHOULIS, J. NELSON, D. D. C. BRADLEY
Center for Electronic Materials and Devices, Department of Physics, Blackett Laboratory, Imperial College London, Prince Consort Road, London SW7 2BW, UK
E-mail: y.kim@ic.ac.uk

S. COOK, J. R. DURRANT
Center for Electronic Materials and Devices, Department of Chemistry, Imperial College London, Exhibition Road, London SW7 2AZ, UK

We have fabricated organic solar cells with blends of regioregular poly(3-hexylthiophene) (P3HT) and 1-(3-methoxycarbonyl)-propyl-1-phenyl-(6,6)C_{61} (PCBM) as electron donor and electron acceptor, respectively. Blend composition and device annealing effects were investigated with optical absorption and photoluminescence spectroscopy, atomic force microscopy, photocurrent spectroscopy, and current-voltage characteristic measurements on devices under monochromatic or air mass (AM) 1.5 simulated solar light illumination. The highest efficiency was achieved for the 1:1 (P3HT:PCBM) weight ratio composition. The good performance is attributed to an optimized morphology that enables close intermolecular packing of P3HT chains. Inferior performance for the 1:2 composition is attributed to poorer intermolecular packing with increased PCBM content, while phase segregation on a sub-micron scale was observed for the 1:4 composition. The power conversion efficiency (AM 1.5) was doubled by the thermal annealing of devices at 140°C to reach a value of 1.4%.

1. Introduction

Efficient photoinduced charge separation at donor-acceptor interfaces has been reported for blends of electron-donating conjugated polymers and electron-accepting organic molecules [1, 2]. The highest quantum efficiencies have been achieved for the so-called "bulk heterojunction structure" where intimate mixing of electron-donating (*p*-type) and electron-accepting (*n*-type) molecules leads to the formation of microscopic heterojunctions between domains of the two materials, throughout the bulk film. Promising early results have generated much interest in developing photovoltaic cells and photodiodes with this bulk heterojunction structure because of the benefits of a simple device structure, ease of processability, device flexibility, and the prospect of low cost manufacturing [3–5].

The most representative bulk heterojunction structures reported to date consist of blends of poly[2-methoxy-5-(3′,7′-dimethyloctyloxy)-1,4-phenylene-vinylene] (MDMO-PPV or OC_1C_{10}-PPV) and 1-(3-methoxycarbonyl)-propyl-1-phenyl-(6,6)C_{61} or [6,6]-phenyl C_{61}-butyric acid methyl ester (PCBM), from which power conversion efficiencies of 2.5–3% have been achieved under air mass (AM) 1.5 simulated solar energy illumination [4, 7]. These high efficiencies are attributed to effective control of morphology through the choice of solvent and composition, as well as to electrode modification (LiF insertion) to assist electron collection [6–8]. Further improvements have been made using C_{70}-PCBM that exhibits much better light harvesting than PCBM at longer wavelengths [9].

Recently much higher external quantum efficiencies and power conversion efficiencies have been reported for bulk heterojunction solar cells made from blends of poly(3-hexylthiophene) (P3HT) and PCBM. Maximum efficiencies were achieved with the aid of thermal annealing and/or electrical aging of devices [10, 11]. However, the effect of the blend composition has not yet been reported in any detail for P3HT:PCBM bulk heterojunction solar cells. Device performance has been reported for only two compositions, namely weight ratios of 1:2 and 1:3 (P3HT:PCBM) [10, 11]. No clear information has been given on the influence of the molecular weight and regioregularity of the P3HT or on the effect of different solvents [10, 11].

In this work we report the effect of composition on the performance of bulk heterojunction solar cells made from blend films of regioregular P3HT and PCBM that are prepared using chlorobenzene as the solvent. In addition, the effect of annealing devices at various temperatures was investigated. We find that the 1:1 (P3HT:PCBM) weight ratio composition shows the

*Author to whom all correspondence should be addressed.

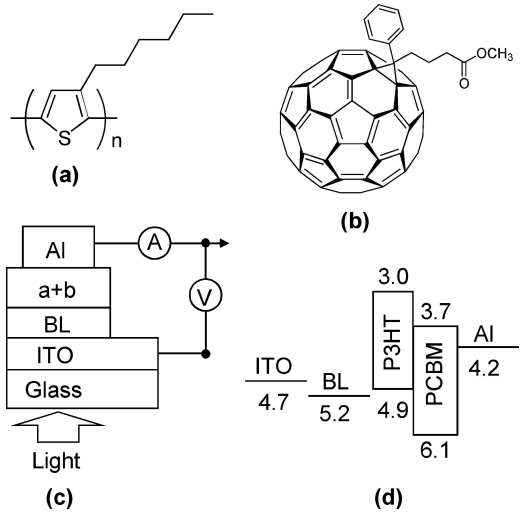

Figure 1 Chemical structure of (a) P3HT and (b) PCBM, (c) cross-sectional view of organic photovoltaic device, and (d) flat energy band diagram: 'BL' denotes a PEDOT:PSS layer.

highest power conversion efficiency while further increasing the PCBM content reduces the efficiency. Device annealing at 140°C doubles the power conversion efficiency (AM 1.5) of as-fabricated devices to reach 1.4%.

2. Experimental procedures

2.1. Materials and solutions

Regioregular P3HT was synthesized by Merck Chemicals Ltd. The typical weight and number average molecular weights were 4.4×10^4 and 2.8×10^4, respectively [12]. Regioregularity greater than 96% was measured by nuclear magnetic resonance spectroscopy. The concentration of residual metallic impurities (mostly Ni and Mg) was less than 10 μg/g. PCBM was used as received from the University of Groningen, The Netherlands. The chemical structures of P3HT and PCBM are shown in Fig. 1. Blend solutions with various compositions (P3HT:PCBM = 1:0, 1:0.1, 1:0.5, 1:1, 1:2, and 1:4 weight ratios) were prepared in chlorobenzene at a solution concentration of 30 mg/ml. These solutions were vigorously stirred for more than 24 h at room temperature to maximise mixing. All resulted in homogeneous solutions except for the 1:4 composition that showed phase separation in solution which was visible to the naked eye.

2.2. Film and device fabrication

The pristine polymer and blend solutions were spin-coated onto quartz substrates for ultraviolet-visible (UV-vis) absorption and photoluminescence (PL) measurements. The same solutions were spin-coated onto glass slides for atomic force microscopy (AFM) measurements. For solar cell fabrication ITO coated glass substrates (~25 Ω/cm^2) were cleaned with acetone and isopropyl alcohol several times and then dried with flowing nitrogen. On top of the cleaned ITO glass, a poly(3,4-ethylenedioxythiophene): poly(styrenesulfonate) (PEDOT:PSS) (Baytron P VP AI 4083 grade, HC Stark) layer was spin-coated, before being soft-baked at 110°C for 15 min. Next, the P3HT:PCBM blend films were spin-coated on the PEDOT:PSS layer at 2000–2500 rpm. After spin-coating all blend films were "soft-baked" at 50°C for 30 min to remove any residual solvent. Finally a ~1500 Å thick aluminium layer was deposited on the soft-baked blend films by thermal evaporation at $\sim 3 \times 10^{-6}$ Torr, defining an active area of 4.5 mm^2 (see Fig. 1). Device annealing was carried out in ambient air at various temperatures from room temperature to 230°C for 4 min.

2.3. Measurements

The optical absorption and PL spectra of pristine P3HT and blend films were measured using an UV-vis spectrophotometer (Unicam, Analytical Technology, Inc.) and spectrofluorimeter (FluoroMax-3, Jobin-Yvon), respectively. An atomic force microscope (AFM, Burleigh Instruments) and optical microscope (Zeiss, Axioplan) were used to measure the surface and bulk morphology of blend films, respectively. The photovoltaic characteristics of devices under monochromatic light illumination were measured using a system equipped with an electrometer (Keithley 237), a monochromater (Oriel CVI CM110), and a Xe lamp (150 W), while the device performance under white light illumination (AM1.5) was measured using a home built solar simulator based on a filtered Xe lamp with output intensity of 100 mW/cm^2 (Costronics Electronics).

3. Results and discussion

3.1. Optical property of blend films

Fig. 2 shows the optical density of pristine P3HT and blend films. As the PCBM content increases up to the 1:1 composition, the optical density at the wavelengths between 570 and 650 nm decreases whereas that below

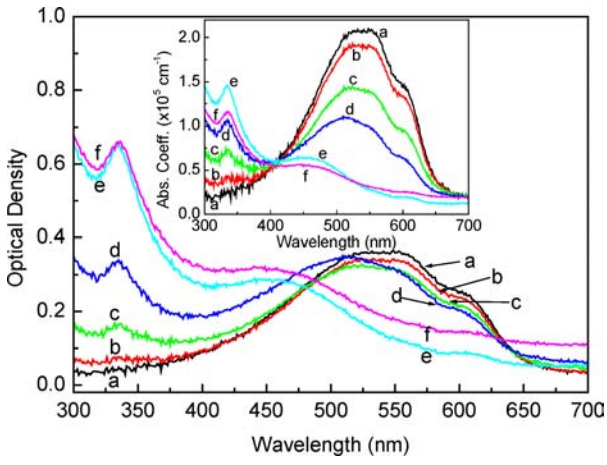

Figure 2 Optical density and absorption coefficient of P3HT:PCBM blend films: P3HT:PCBM (weight ratio) = 1:0 (a), 1:0.1 (b), 1:0.5 (c), 1:1 (d), 1:2 (e), and 1:4 (f). The film thickness of (a), (b), (c), (d), (e), and (f) is 40 nm, 41 nm, 52 nm, 73 nm, 102 nm, and 131 nm, respectively: Here it should be noted that the thickness of (e) and (f) films was averaged between minimum and maximum values because of very rough film surface morphology.

480 nm grows gradually. Further increasing the PCBM content leads to a qualitative change in spectral shape. These trends are clearly shown in the absorption coefficient spectra (see inset to Fig. 2). The spectral shape of the pristine P3HT absorption is preserved in the blends up to the 1:1 composition, while the falling magnitude of the absorption coefficient at wavelengths longer than 400 nm can be attributed to the reduction in the volume occupied by P3HT. This indicates that the self organization or intermolecular packing structure of the P3HT chains is preserved over this range of compositions. However, for the two higher PCBM content, the red band of the P3HT absorption is strongly quenched while absorption in the blue region is maintained. This suggests that the dilution of P3HT molecules by the presence of PCBM molecules has disrupted the intermolecular packing structure of the P3HT chains and reduced the density of aggregates that give rise to the red absorption. Light harvesting at the longer wavelengths is therefore expected to be poor for high PCBM content blends.

Fig. 3 shows the PL intensity for blend films of different PCBM content. The PL intensity decreases strongly upon adding approximately 10 wt.% PCBM (1:0.1 composition) to pristine P3HT, and shows a minimum at the 1:2 composition where the PL intensity is then only 1.5% of its maximum value for P3HT alone. This significant reduction in the PL intensity is attributed to efficient photoinduced charge separation between electron-donating (P3HT) and electron-accepting (PCBM) molecules [13, 14]. Up to the 1:1 composition the PL spectrum is similar in shape to that of pristine P3HT (see inset to Fig. 3), indicating that the PL is due to photogenerated excitons in P3HT that do not take part in charge separation. The strong PL quenching for the 1:2 composition indicates that most of the P3HT excitons are involved in the charge separation process at this composition. The increase in PL intensity for the 1:4 composition is due to PL from PCBM domains, as is evident from the characteristic luminescence at 720 nm [8].

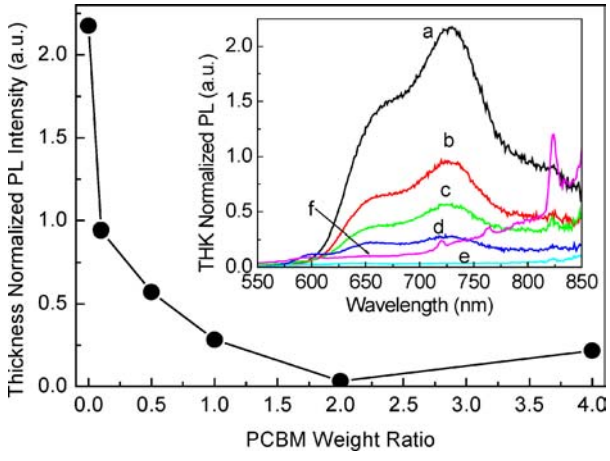

Figure 3 Thickness normalized PL intensity of P3HT:PCBM blend films at 730 nm as a function of PCBM weight ratio. Inset shows the thickness normalized PL spectra: P3HT:PCBM (weight ratio) = 1:0 (a), 1:0.1 (b), 1:0.5 (c), 1:1 (d), 1:2 (e), and 1:4 (f). The excitation wavelength was 480 nm.

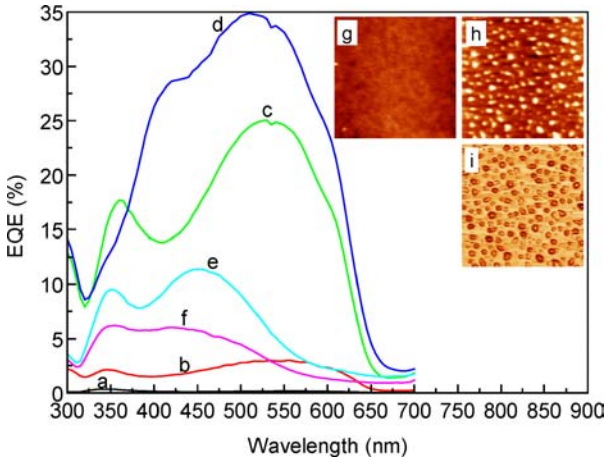

Figure 4 EQE spectra of the devices with P3HT:PCBM blend films: P3HT:PCBM (weight ratio) = 1:0 (a), 1:0.1 (b), 1:0.5 (c), 1:1 (d), 1:2 (e), and 1:4 (f). The incident light intensity at 480 nm was 6.2 mW/cm^2. The inset shows AFM images (5 μm × 5 μm size) of P3HT:PCBM blend films: P3HT:PCBM (weight ratio) = 1:1 (g), 1:4 (h), and a cosine filtered image for the 1:4 blend film (i).

3.2. External photocurrent quantum efficiency spectra and film morphology

Although the 1:2 composition showed the minimum PL intensity, which in turn normally indicates the most efficient charge separation, the maximum external photocurrent quantum efficiency was achieved for the 1:1 composition (see Fig. 4). This can be explained by the difference in absorption coefficients that the blends possess, as shown in Fig. 2. The improved light harvesting by the 1:1 blend relative to the 1:2 blend compensates for the less efficient charge separation. In contrast, the higher external quantum efficiency for the 1:4 composition than the 1:0.1 composition in the 420–520 nm range shows that the improved charge separation for the 1:4 blend relative to the 1:0.1 blend compensates for the less efficient light harvesting. It can be seen, therefore, that both the light harvesting and charge separation efficiencies are important for high photocurrent quantum efficiency and both need to be optimized for best performance.

AFM images of the film morphology of blend films with 1:1 and 1:4 compositions are shown in the inset to Fig. 4. The 1:1 composition shows almost no phase segregation within the measurement resolution whereas submicron-sized particles are observed for the 1:4 composition. In case of the 1:2 composition (not shown here), the surface morphology was slightly coarser than the 1:1 composition [16]. Such composition dependent morphology has previously been observed for blends of MDMO-PPV and PCBM [8]. For that material system it has been established that a fairly homogenous blend is obtained for PCBM contents up to 50% by weight, and that at higher PCBM content, PCBM-rich domains begin to segregate. By considering both the morphology and the absorption coefficient for the 1:4 composition, we deduce that the P3HT chains are well mixed with PCBM molecules, leading to suppressed intermolecular packing of P3HT chains, but the excess PCBM molecules form a second, PCBM-rich, phase that gives rise to the large scale phase segregation.

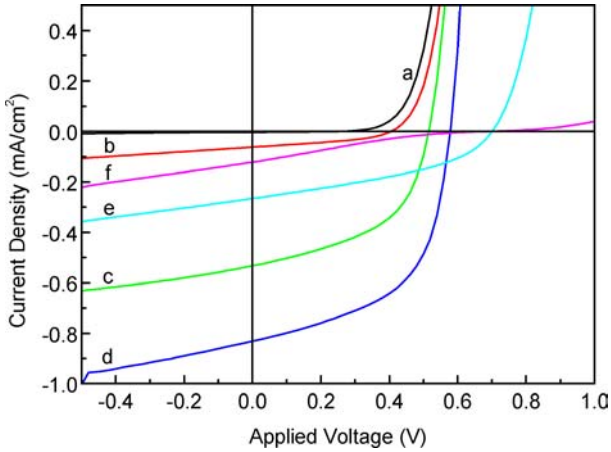

Figure 5 Current density as a function of applied voltage for the devices with P3HT:PCBM blend films: P3HT:PCBM (weight ratio) = 1:0 (a), 1:0.1 (b), 1:0.5 (c), 1:1 (d), 1:2 (e), and 1:4 (f). Measurements were performed under monochromatic light (480 nm) excitation with an intensity of 6.2 mW/cm^2.

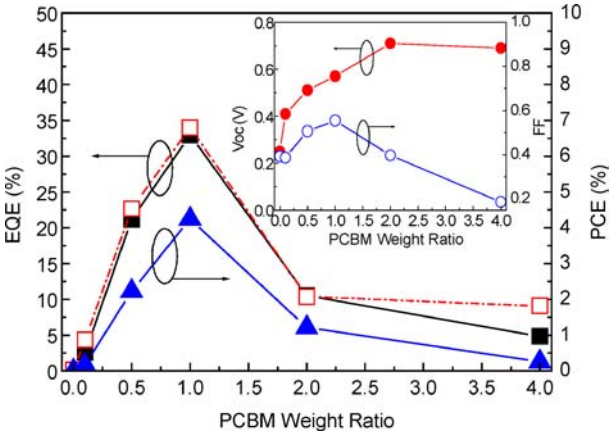

Figure 6 EQE (filled square: under 6.2 mW/cm^2 at 480 nm; open square: under 0.03 mW/cm^2 at 480 nm) and PCE (filled triangle: under 6.2 mW/cm^2 at 480 nm) for devices with P3HT:PCBM blend films as a function of PCBM weight ratio. The inset shows the open circuit voltage and fill factor as a function of PCBM weight fraction: Measurements were performed under monochromatic light (480 nm) excitation with an intensity of 6.2 mW/cm^2.

These PCBM rich domains may assist charge collection in high PCBM content blends, owing to the high electron mobility in PCBM [15], which helps to compensate for poor light harvesting.

3.3. Device performance under monochromatic light illumination

Current-voltage characteristics of devices under monochromatic light illumination (480 nm) are shown in Fig. 5. The shape of the current-voltage curves is similar for the compositions from 1:0 to 1:1, showing a gradual increase in both short circuit current density (J_{sc}) and open circuit voltage (V_{oc}) with increasing PCBM content. At higher PCBM content, the J_{sc} decreases significantly whereas the V_{oc} continues to increase up to 1:2 composition. These variations in J_{sc} can be attributed largely to the variations in absorption coefficient and charge separation efficiency. In addition, the slight thickness increase of blend films is considered to be partly responsible for the J_{sc} and V_{oc} increase due to the increased photogeneration rate. However, the increase in V_{oc} is still harder to explain in this system compared to MDMO-PPV:PCBM devices. Studies on MDMO-PPV:PCBM devices show that introduction of PCBM tends to reduce the V_{oc} compared to the pristine polymer device, and that V_{oc} is composition independent for PCBM contents above about 10% by weight [8, 17]. In the case of P3HT, possible explanations for the variation in V_{oc} may include the effect of PCBM content on the chain packing near to the electrodes and its effect on recombination. In the case of the 1:4 composition, the coarse film morphology may be responsible for the abnormal current-voltage curve shape, that typically arises from bottlenecks in charge transfer within the active layer or between active layers and electrodes [18].

It was shown in Fig. 4 above that as the PCBM content increases, the external quantum efficiency increases up to the 1:1 composition and then decreases. In Fig. 6, the external quantum efficiency at 480 nm and incident light intensities of 0.03 and 6.2 mW cm^{-2} are plotted as a function of PCBM content. The trend corresponds with the trend in J_{sc} shown in Fig. 5 and roughly with the trend in absorption coefficient shown in Fig. 2. Fig. 6 also shows that for all compositions except the 1:4 composition, the external quantum efficiency is almost independent of incident light intensity over more than two orders of magnitude. This indicates that the short-circuit photocurrent generation of these P3HT:PCBM blend devices is not strongly limited by bimolecular charge recombination, because dominant bimolecular recombination leads to a sublinear dependence of EQE on light intensity. In the case of the 1:4 composition the strong effect of light intensity may indicate stronger recombination. The power conversion efficiency follows a similar trend to the external quantum efficiency but not to the V_{oc} (see inset to Fig. 6), and therefore is apparently dominated by the short circuit photocurrent generation.

In order to examine the morphological quality of our blend films, we calculated the morphology parameter, β, from the slope of short circuit current versus incident light intensity [16]. As explained in Ref. 16, a β value greater than 0 expresses the rate at which the EQE decreases with increasing light intensity. High β values may be expected for coarse morphologies where bimolecular recombination is dominant. As shown in Fig. 7, large β values are obtained for the 1:0.1 and 1:4 compositions, namely the extreme compositions where one component is predominant over the other. For the 1:4 composition the β measurement is in good agreement with the coarse morphology, as reported earlier [16]. As a result, the external quantum efficiency decreases more swiftly for these two extreme compositions as the incident light intensity increases (see inset to Fig. 7). However, the relationship between β and film morphology should be further investigated for the 1:0.1 composition.

3.4. Device annealing effects

Fig. 8 shows the current-voltage characteristics of devices made from blends of composition 1:1, before

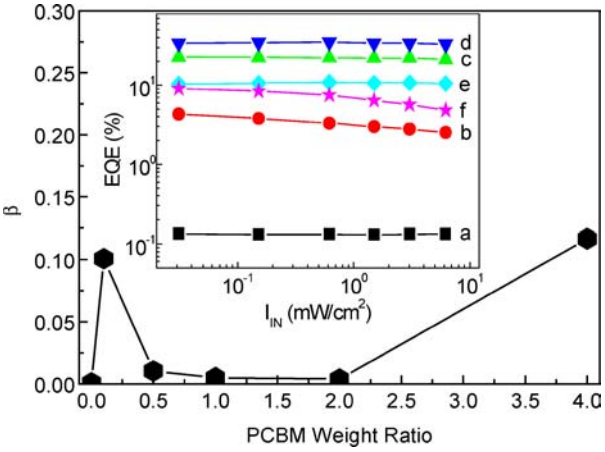

Figure 7 β values for devices with P3HT:PCBM blend films as a function of PCBM weight fraction. The inset shows the incident light intensity dependence of the EQE: P3HT:PCBM (weight ratio) = 1:0 (a), 1:0.1 (b), 1:0.5 (c), 1:1 (d), 1:2 (e), and 1:4 (f). Measurements were performed under monochromatic light (480 nm) excitation with an intensity of 6.2 mW/cm^2.

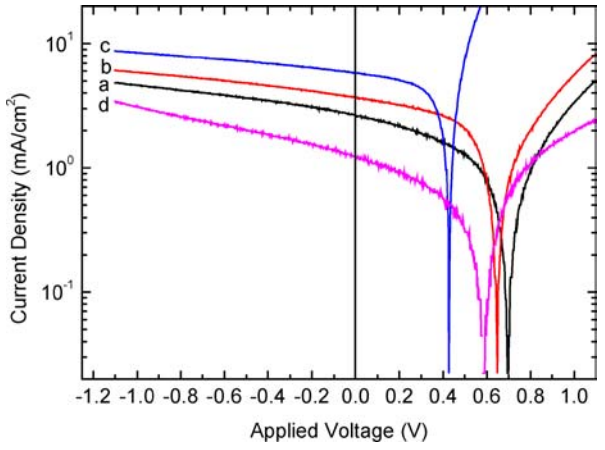

Figure 8 Current density as a function of applied voltage for devices with P3HT:PCBM (1:1 by weight) blend films: (a) As-fabricated device, (b) annealed at 50°C, (c) annealed at 140°C, and (d) annealed at 230°C. The P3HT:PCBM film thickness before annealing was ~70 nm for all devices. The device annealing time and environment were 4 min and in air, respectively. Measurements were performed under AM 1.5 simulated white light with an intensity of 100 mW/cm^2.

and after thermal annealing. Upon thermal annealing up to 140°C the fill factor of the current-voltage curve improves. This may be evidence of better charge carrier mobilities, leading to reduced recombination, or of reduced shunt paths inside the blend films. However, further annealing at 230°C degrades the shape of the current-voltage curve to that of the as-prepared device, suggesting that the film morphology may have been degraded.

Fig. 9 shows the photovoltaic device performance parameters as a function of annealing temperature. Both J_{sc} and the power conversion efficiency increase for temperatures up to 140°C and then decrease. This J_{sc} increase is attributed to a better packing of P3HT chains as well as a structural reorganization of the blend film. The maximum power conversion efficiency reached is 1.4%. The fill factor shows a similar trend to the power conversion efficiency, whereas the V_{oc} shows the opposite trend.

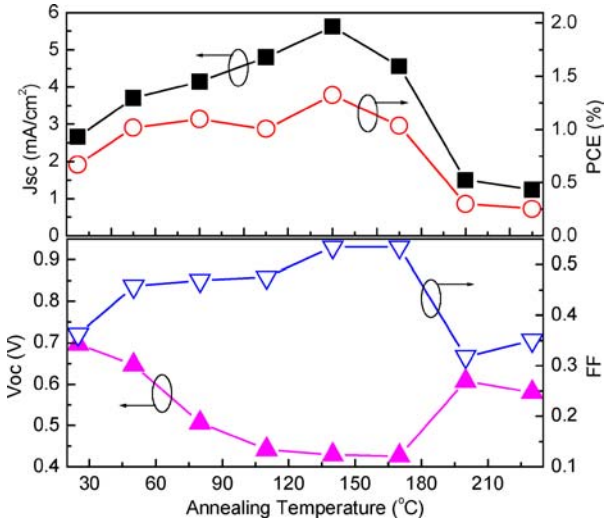

Figure 9 Short circuit current, PCE, open circuit voltage, and fill factor for P3HT:PCBM (1:1 by weight) blend film devices as a function of annealing time. Measurements were performed under AM 1.5 simulated white light with an intensity of 100 mW/cm^2.

The reason for the reduction in V_{oc} is not clear, but it may be due to the reorganization of P3HT chains relative to the PEDOT:PSS electrode. One driving force for this reorganization at a temperature below the glass transition of P3HT chains (~110°C) is the ageing effect on non-equilibrium morphologies that result from the spin-coating: The film morphology quickly freezes on rapid evaporation of solvent molecules and the polymer chains are subject to shear forces. Another driving force, at temperatures above the P3HT glass transition, is the movement of both P3HT chains and PCBM molecules due to the thermal transition of P3HT chains. At much higher temperature than the glass transition, close to the melting point of P3HT (230°C), the vigorous vibrational and translational movement of P3HT chains leads to more complex morphologies between P3HT and PCBM molecules, and to a poorly organized geometry.

On the basis of the results of our thermal annealing experiments in air, we have achieved a further optimization to ~3% power conversion efficiency with the same device structure by undertaking thermal annealing at 140°C but in a nitrogen atmosphere [19]. In order to try and explain the detailed mechanism for the annealing improvements we have studied, the associated charges in dark current-voltage characteristics as well as EQE spectra are reported elsewhere (ref. 20).

4. Conclusion

The effect of blend composition and device annealing was studied for organic solar cells with blend films of regioregular P3HT and PCBM. The highest external quantum and power conversion efficiencies were achieved for a 1:1 composition by weight. There then appears to be a good balance between having a suitable morphology for charge separation, and good light harvesting properties at longer wavelengths. Further addition of PCBM molecules (1:2 and 1:4 compositions) significantly reduced the efficiency. This was

tentatively attributed to a resulting disruption of intermolecular packing for the P3HT chains so that the light absorption at longer wavelengths was largely decreased. Other explanations are also being considered. Device annealing is likely to enhance the charge carrier mobility as shown by the better fill factor in the current-voltage curves. The highest power conversion efficiency (~1.4%) was achieved by annealing devices at 140°C in air. However further annealing at higher than this critical temperature reduced the efficiency.

Acknowledgements

The authors thank Merck Chemicals Ltd. for supplying the P3HT polymer and British Petroleum for financial support.

References

1. N. S. SARICIFTCI, L. SMILOWITZ, A. J. HEEGER and F. WUDL, *Science* **258** (1992) 1474.
2. J. J. M. HALLS, C. A. WALSH, N. C. GREENHAM, E. A. MAESEGLIA, R. H. FRIEND, S. C. MORATTI and A. B. HOLMES, *Nature* **376** (1995) 498.
3. G. YU, J. GAO, J. C. HUMMELEN, F. WUDL and A. J. HEEGER, *Science* **270** (1995) 1789.
4. C. J. BRABEC, N. S. SARICIFTCI and J. C. HUMMELEN, *Adv. Funct. Mater.* **11** (2001) 15.
5. J. NELSON, *Curr. Opin. Solid State Mater. Sci.* **6** (2002) 87.
6. S. E. SHAHEEN, C. J. BRABEC, N. S. SARICIFTCI, F. PADINGER, T. FROMHERTZ and J. C. HUMMELEN, *Appl. Phys. Lett.* **78** (2001) 841.
7. C. J. BRABEC, S. E. SHAHEEN, C. WINDER, N. S. SARICIFTCI and P. DENK, *ibid.* **80** (2002) 1288.
8. J. K. J. VAN DUREN, X. YANG, J. LOOS, C. W. T. BULLE-LIEUWMA, A. B. SIEVAL, J. C. HUMMELEN and R. A. J. JANSSEN, *Adv. Funct. Mater.* **14** (2004) 425.
9. M. M. WIENK, J. M. KROON, W. J. H. VERHEES, J. KNOL, J. C. HUMMELEN, P. A. VAN HAL and R. A. J. JANSSEN, *Angew. Chem. Int. Ed.* **42** (2003) 3371.
10. P. SCHILINSKY, C. WALDAUF and C. J. BRABEC, *Appl. Phys. Lett.* **81** (2002) 3885.
11. F. PADINGER, R. S. RITTBERGER and N. S. SARICIFTCI, *Adv. Funct. Mater.* **13** (2003) 85.
12. Y. KIM, M. GILES, I. MCCULLOCH and D. D. C. BRADLEY, *Private Communications* (2002).
13. H. J. SNAITH, A. C. ARIAS, A. C. MORTEANI, C. SILVA and R. H. FRIEND, *Nano Lett.* **2** (2002) 1353.
14. Y. KIM, S. COOK, S. A. CHOULIS, J. NELSON, J. R. DURRANT and D. D. C. BRADLEY, *Chem. Mater.* **16** (2004) 4812.
15. V. D. MIHAILETCHI, J. K. J. VAN DURREN, P. W. M. BLOM, J. C. HUMMELEN, R. A. J. JANSSEN, J. M. KROON, M. T. RISPENS, W. J. H. VERHEES and M. M. WIENK, *Adv. Funct. Mater.* **13** (2003) 43.
16. Y. KIM, S. COOK, S. A. CHOULIS, J. NELSON, J. R. DURRANT and D. D. C. BRADLEY, *Ibid.*, to be submitted (2004).
17. M. C. SCHARBER, N. A. SCHULTZ, N. S. SARICIFTCI and C. J. BRABEC, *Phys. Rev. B.* **67** (2003) 085202.
18. J. NELSON, J. KIRKPATRICK and P. RAVIRAJAN, *ibid.* **69** (2003) 035337.
19. Y. KIM, S. COOK, S. A. CHOULIS, J. NELSON, J. R. DURRANT and D. D. C. BRADLEY, *Appl. Phys. Lett.*, in print (2005).
20. Y. KIM, S. COOK, S. A. CHOULIS, J. NELSON, J. R. DURRANT and D. D. C. BRADLEY, *Phys. Rev. B*, to be submitted (2004).